PHYSICAL REVIEW A **89**, 041401(R) (2014)

Magneto-optical trapping of holmium atoms

J. Miao, J. Hostetter, G. Stratis, and M. Saffman
Department of Physics, University of Wisconsin, 1150 University Avenue, Madison, Wisconsin 53706
(Received 16 January 2014; published 3 April 2014)

We demonstrate sub-Doppler laser cooling and magneto-optical trapping of the rare-earth element holmium. Atoms are loaded from an atomic beam source and captured in six-beam $\sigma_+ - \sigma_-$ molasses using a strong $J = 15/2 \leftrightarrow J = 17/2$ cycling transition at $\lambda = 410.5$ nm. Due to the small difference in hyperfine splittings and Landé g factors in the lower and upper levels of the cooling transition the MOT is self-repumped without additional repump light, and deep sub-Doppler cooling is achieved with the magnetic trap turned on. We measure the leakage out of the cycling transition to metastable states and find a branching ratio $<10^{-5}$, which is adequate for state-resolved measurements on hyperfine encoded qubits.

DOI: 10.1103/PhysRevA.89.041401 PACS number(s): 37.10.De, 37.10.Jk, 03.67.Lx

The magneto-optical trap (MOT) is a standard and very widely used tool in cold-atom physics. To date MOT operation has been demonstrated for about 30 different neutral elements. Operation of a MOT on an open transition which allows for pumping into metastable states which are not cooled requires "repump" light to return the atomic population to the levels participating in laser cooling. The rare-earth lanthanides did not originally appear amenable to laser cooling due to the presence of an open f shell (except for Yb which was laser cooled in 1999 [1]) and a correspondingly complex atomic structure. It was recognized by McClelland that the lanthanides are amenable to laser cooling due to the presence of cycling transitions between odd (even) parity ground states with angular momentum J and even (odd) parity excited states with angular momentum $J' = J + 1$. MOT operation was first demonstrated with an open-f-shell lanthanide in 2006 using Er [2]. That demonstration was followed in 2010 by demonstration of MOTs for Dy [3] and Tm [4]. In this Rapid Communication we report on the operation of a Ho MOT loaded from an atomic beam with and without laser slowing [5]. The Doyle group has also recently demonstrated lanthanide MOTs including Ho using buffer-gas precooling of an atomic beam [6].

Interest in laser cooling and trapping of lanthanide atoms is motivated by several topics in current research. Quantum degenerate bosonic and fermionic gases of Dy [7,8] and Er [9,10] open up new research directions due to the large magnetic moments Er ($7\mu_B$) and Dy ($10\mu_B$) which provide for much stronger dipolar magnetic interactions between neutral atoms than are present in the more widely studied alkali gases. Ho has one stable isotope, ^{165}Ho, which is bosonic with a nuclear spin of $I_{nuc} = 7/2$ and a ground electronic configuration $[\mathrm{Xe}]4f^{11}6s^2$. The ground-state term is $^4I^\circ, J = \frac{15}{2}$, giving eight hyperfine levels, $F_g = 4, \ldots, 11$, and the magnetic moment is $9\mu_B$. Ho is distinguished by having 128 hyperfine Zeeman states, the largest number of any stable atomic isotope. This large number of states is of interest for collective encoding of multiqubit quantum registers [11,12]. Implementation of collective encoding will rely on Rydberg blockade interactions [13] in a dense atomic sample. The demonstration of sub-Doppler laser cooling, MOT operation, and optical cycling transitions with fractional leakage rates at the 10^{-5} level reported here are first steps towards Rydberg spectroscopy and qubit encoding in Ho atoms.

The level diagram of Ho together with cycling transitions suitable for cooling is shown in Fig. 1. The ground state has $J = 15/2$ with odd parity. There are eight dipole-allowed transitions at wavelengths longer than 410 nm to levels with even parity and $J = 17/2$. Since there are no odd-parity levels with $15/2 \leqslant J \leqslant 19/2$ in between the ground state and the upper levels of the six transitions labeled 1–6, these transitions are cycling. Relevant transition parameters are given in Table I. The 410.5-nm transition from the ground state to $|e\rangle = [\mathrm{Xe}]4f^{11}6s6p(^1P), J = 17/2$ at 24 361 cm^{-1} (labeled 9 in Fig. 1) is not cycling since there are odd-parity levels above the ground state accessible by electric dipole decay from $|e\rangle$. Nevertheless, a closer examination of the odd-parity levels below $|e\rangle$ with $15/2 \leqslant J \leqslant 19/2$ reveals that almost all possible transitions have $|\Delta j| > 1$ on a single electron or are forbidden due to intercombination spin changes. The only transition which is allowed for single-electron jumps is $|e\rangle - |4f^{11}5d6s(^1D), J = 17/2\rangle$ at a transition energy of 475 cm^{-1}. This transition is very weak due to the ω^3 factor in the expression for the radiative linewidth, with ω being the transition frequency. We can roughly estimate the decay rate using hydrogenic orbitals, which gives $\gamma' \sim 4000.0$ s^{-1}. The actual radial matrix elements are unknown, so this value is not quantitatively correct but provides some guidance. To the extent that LS coupling is a good description for the level structure of Ho we expect that the cooling transition with $|g\rangle$ as an upper level will have small leakage since $\gamma'/\gamma \sim 10^{-5}$.

The experimental apparatus is shown in Fig. 2. A water-cooled effusion cell with Ta crucible operated at $T = 1150\,^\circ$C provides a beam of Ho atoms with a mean velocity of 510 m/s. The atomic beam passes through a 0.25-cm-diameter tube to prevent outflow of any melted Ho from the horizontally oriented effusion cell and a 0.25-cm-diameter aperture for differential pumping before entering the MOT chamber. Two ion pumps provide a base pressure of 10^{-9} mbar in the MOT chamber. A pair of electric coils provides a quadrupole magnetic field with a gradient of up to 0.4 T/m (vertical axis) and 0.2 T/m (horizontal axis). The cooling beams were arranged in a standard six-beam $\sigma_+ - \sigma_-$ configuration. The beams had Gaussian waists ($1/e^2$ intensity radius) of 2.4 mm and total incident power of 40 mW, which was doubled by retroreflecting the beams. The cooling light was detuned by $\Delta_c \sim -1.5\gamma$ from the $F_g = 11 \rightarrow F_e = 12$ cycling transition. Repump

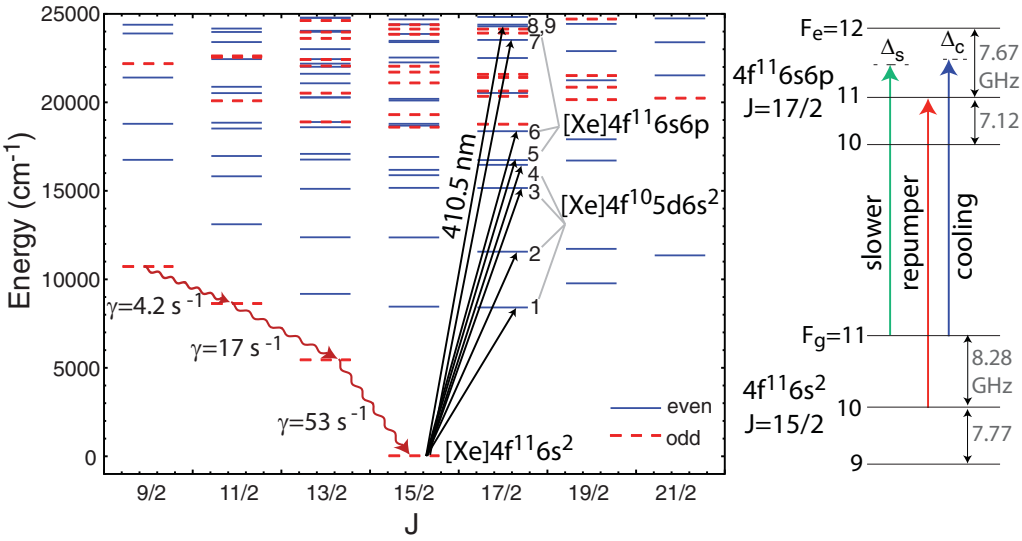

FIG. 1. (Color online) Energy levels of Ho. The upper levels of the cycling and cooling transitions are labeled 1–7. The diagram on the right shows the cooling, repumper, and slowing light used on the 410.5-nm transition to level $|e\rangle$.

light was tuned to $F_g = 10 \rightarrow F_e = 11$ and overlapped with all MOT beams. In addition a circularly polarized slowing beam counterpropagating with the atomic beam was detuned by $\Delta_s = -2\pi \times 320$ MHz from the $F_g = 11 \rightarrow F_e = 12$ transition. The slowing beam had a power of 140 mW and was focused to a waist of 1.0 mm. Measurements of the MOT atom number and density were made with an electron-multiplying charge-coupled-device (EMCCD) camera using either fluorescence imaging or absorption imaging with an additional beam tuned to be resonant with the cooling transition. All laser beams were derived from a frequency-doubled Ti:sapphire laser (M^2 Solstis with ECD-X) providing up to 1.5 W of 410.5-nm light. The laser was locked to the cooling transition using saturation spectroscopy in a hollow cathode lamp. The frequency and power level of the cooling, repump, and slowing light were controlled by acousto-optic modulators.

The hyperfine energies shown in Fig. 1 were calculated from known values of the A and B constants for the ground state [18] and measured values for the excited state. We measured the hyperfine constants of the upper level of the cooling transition using modulation transfer spectroscopy in the hollow cathode lamp. Fits to our data gave $A = 654.9 \pm 0.3, B = -620 \pm 20$ MHz. These values agree well with earlier measurements reported in [19].

With the slowing beam turned on but no repump light, we achieved a typical MOT population of $N \sim 1.5 \times 10^4$ and atomic density of $n_a \sim 6.5 \times 10^{14}$ m^{-3}, as shown in Fig. 3. Additional data taken with 290 mW of MOT light, beam waists of 1.1 cm, and 38 mW of slower light gave larger MOTs with up to $N = 2 \times 10^5$ atoms.

The atom number measurements were calibrated by integrating the detected EMCCD MOT image using the measured camera sensitivity to 410.5-nm light and an integration time of 50 ms. The measurement relies on knowing the rate of scattered photons per atom, which we estimated by the two-level expression [20]

$$r = \gamma \rho_{ee} = \frac{\gamma}{2} \frac{I_T/I_s}{1 + 4\Delta_c^2/\gamma^2 + I_T/I_s}. \quad (1)$$

TABLE I. Ho cycling and cooling transitions. The columns list the vacuum wavelength, natural linewidth, and Doppler cooling limit ($T_D = \hbar\gamma/2k_B$). Wavelengths are calculated from [14].

Transition	λ (nm)	$\gamma/2\pi$ (MHz)	Doppler limit (μK)
1	1193.0	unknown	
2	867.3	unknown	
3	660.9	unknown	
4	608.3	0.038[a]	0.91
5	598.5	0.146[b,c]	3.5
6	545.3	unknown	
7	425.6	1.59[b,c]	38.0
8[d]	412.1	2.3[b,c]	55.0
9	410.5	32.5[b,c]	780.0

[a]Linewidth derived from oscillator strength value reported in [15].
[b]Reference [16].
[c]Reference [17].
[d]Two-electron jump transition.

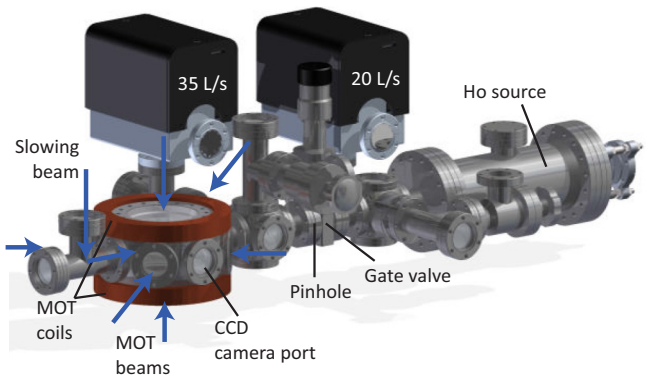

FIG. 2. (Color online) Vacuum and laser cooling setup. The length of the apparatus from end to end is about 1 m. The slowing beam enters the vacuum chamber through a vertical window and is reflected from a Cu mirror to propagate towards the atomic source.

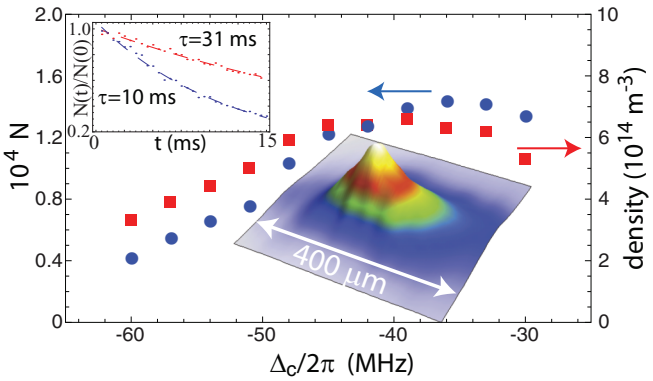

FIG. 3. (Color online) Number of trapped atoms (circles) and peak density (squares) as a function of cooling-light detuning with the slower light turned on and the repump light turned off. The magnetic-field gradient was 0.3 T/m. The insets show an averaged fluorescence image of the trapped atoms from 100 exposures at −36 MHz detuning and population decay curves with exponential fits at −15 MHz (fast decay) and −45 MHz (slow decay).

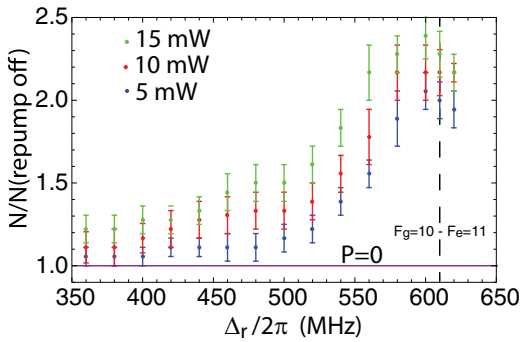

FIG. 4. (Color online) MOT population as a function of repumper detuning relative to the $F_g = 11 \rightarrow F_e = 12$ transition and repumper power, with the slowing beam off. The population is normalized to the value with no repumper. The data stop at 620 MHz, which was the limit of the acousto-optic modulator used for frequency shifting.

Here ρ_{ee} is the excited state fraction, I_T is the total intensity of the six MOT beams, and for the saturation intensity we use $I_s = 2.76 I_{sc}$. Here $I_{sc} = 614.0\ \mathrm{W/m^2}$ is the saturation intensity for the cycling transition $|F_g = 11, M = 11\rangle \leftrightarrow |F_e = 12, M = 12\rangle$, and the factor of $2.76 = 3(2 \times 11 + 1)/(2 \times 11 + 3)$ accounts for averaging over Zeeman substates and the random light polarization in the MOT region. The scattered light was collected with a lens with a numerical aperture of 0.05 and imaged onto a calibrated electron-multiplying charge-coupled-device camera which allowed us to deduce the atom number on the basis of the camera photoelectron counts.

When the repumper was turned on tuned to the $F_g = 10 \rightarrow F_e = 11$ transition, the atom number values in Fig. 3 increased by less than 1%. The negligible influence of the repump light is due to the fact that the cooling light also repumps the population in $F_g = 10$ much faster than the depumping rate out of $F_g = 11$. The depumping rate due to Raman transitions via $F_e = 10$ or 11 is calculated by averaging over M levels and light polarization and accounting for the branching ratios of the fluorescence decay. We find

$$r_R = \gamma^3 \left[\frac{105}{69938 \Delta^2_{F_e = F_g}} + \frac{455}{17904128 \Delta^2_{F_e = F_g - 1}} \right] \frac{I_T}{I_{sc}}. \qquad (2)$$

In this expression $F_g = 11$ is the F value for the lower level of the cycling transition, $\Delta_{F_e=F_g} = \Delta_{(F+1)_e, F_e} + \Delta_c$, $\Delta_{F_e=F_g-1} = \Delta_{(F+1)_e,(F-1)_e} + \Delta_c$ are the detunings of the MOT light from $F_e = 11$ and $F_e = 10$, and we have assumed the light is far detuned so that we may replace factors of $(1 + 4\Delta^2/\gamma^2 + I_T/I_s)^{-1}$ by $\gamma^2/(4\Delta^2)$. The excited-state hyperfine splittings shown in Fig. 1 are $\Delta_{12,11} = 2\pi \times 7.67$ GHz and $\Delta_{12,10} = 2\pi \times 14.79$ GHz. We find that for $\Delta_c = -2\gamma$, the largest detuning we have used, $r_R = 80\ \mathrm{s^{-1}}$ and $r_R/r = 3.3 \times 10^{-6}$. There is also depumping due to leakage to metastable states. The rate for this process we estimate below to be negligible compared to the Raman rate. The total depumping rate is therefore $<100\ \mathrm{s^{-1}}$. This rate is balanced by the repumping rate for the Raman process $F_g = 10 \rightarrow F_e = 11 \rightarrow F_g = 11$. The cooling light is detuned from the $F_g = 10 \rightarrow F_e = 11$ transition by $-610\ \mathrm{MHz} + \Delta_c/2\pi \sim -650\ \mathrm{MHz}$. The resulting repumping rate is about $8 \times 10^5\ \mathrm{s^{-1}}$.

The ratio of the depumping to repumping rates implies that 99.9% of the population is in $F_g = 11$. We verified that turning on a separate repumper increased the atom number by less than 1%, with the resolution limited by the stability of the MOT number measurement. Thus, even without a separate repumper, the atoms are pumped with better than 99% purity into the $F_g = 11$ level. Further pumping into a specific Zeeman sublevel as a starting point for quantum-state control experiments has not been demonstrated but should be straightforward using an additional π polarized beam tuned to $F_g = 11 \rightarrow F_e = 11$ for pumping into $M = 0$, or a σ_+ polarized beam tuned to $F_g = 11 \rightarrow F_e = 12$ for pumping into $M = 11$.

The effect of the repumper is more significant when the MOT is operated without a slowing beam. In this case the MOT captures only a very small fraction of the low-velocity tail of the atomic beam, and the loading rate is reduced by almost three orders of magnitude, resulting in a very small MOT with $N = 40$ atoms, again without a repumper. Turning on the repumper increases N by a factor of up to 2.5, depending on the detuning of the repumper, as shown in Fig. 4. The increase in atom number cannot be due to additional repumping since, as explained above, the cooling light acts as its own repumper. We instead interpret the data as being due to the repump light cooling and trapping additional atoms on the $F_g = 10 \rightarrow F_e = 11$ transition. The high-temperature atomic source creates a beam which we assume to be uniformly distributed among ground Zeeman states. Since there are 23 Zeeman states in $F_g = 11$ and 21 in $F_g = 10$, we expect roughly a factor of 2 increase, which is in reasonable agreement with the data. No such increase is seen when the slower is on since the slower light is only effective for atoms in $F_g = 11$ and the additional loading of unslowed $F_g = 10$ atoms is negligible.

As shown in Fig. 5, we observe deep sub-Doppler cooling well below $T_D = 780\ \mu\mathrm{K}$ using $\sigma_+ - \sigma_-$ MOT beams. Data were acquired by observing MOT expansion and fitting to Gaussian density profiles. The theoretical dependence of the molasses temperature with respect to detuning is

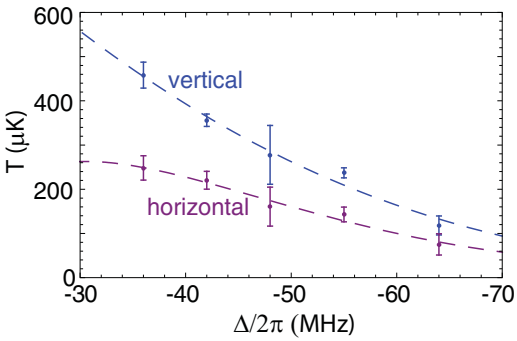

FIG. 5. (Color online) MOT temperature with quadrupole magnetic field on vs detuning at saturation parameter $I/I_s = 1.1$. The temperatures were extracted from fits to time-of-flight data for free expansion times up to 15 ms. The Doppler temperature is 780 μK.

given by [21]

$$T = T_0 + \frac{\hbar\gamma^2}{2k_B|\Delta|}\frac{I}{I_s}\left(a + \frac{b}{1+4\Delta^2/\gamma^2}\right), \tag{3}$$

with a,b being constants and T_0 being the low-intensity temperature limit. The parameters a,b are known for low angular momentum transitions [21] but have not been calculated for the $F_g = 11 \leftrightarrow F_e = 12$ Ho cooling transition. Using separate fit parameters for the horizontal and vertical temperatures, Eq. (3) reproduces the observed dependence on detuning quite well. Cooling anisotropy has also been observed in Dy MOTs [22] and may be due to the large magnetic moments present in rare-earth atoms. Due to the near equality of the g factors of the ground state $F_g = 11$ and excited state $F_e = 12$, 0.82 and 0.83, temperatures reaching ten times below the Doppler limit are achieved with relatively small detunings and with the quadrupole MOT field on during the entire cooling phase.

In order to further study the internal-state dynamics we loaded the MOT to steady state with the slowing beam on and then measured the decay lifetime with the slowing beam turned off, which greatly reduces the loading into the MOT, but the magnetic quadrupole field still on. The MOT population decay can be modeled with the rate equation [23]

$$\frac{dN}{dt} = R_{\rm off} - \Gamma N - \beta N^2. \tag{4}$$

Here $R_{\rm off}$ is the loading rate with the slowing beam off, and the loss rate is $\Gamma = (1-\rho_{ee})\gamma_{\rm bg} + \rho_{ee}(\gamma_{\rm la} + \gamma_{\rm ms})$, where $\gamma_{\rm bg}$ accounts for losses due to background collisions with ground-state atoms, $\gamma_{\rm la}$ is the loss rate due to light-assisted collisions between optically excited and background atoms [24], $\gamma_{\rm ms}$ is the loss rate due to scattering into metastable states, and β accounts for losses from collisions of trapped atoms. Leakage into metastable states may lead to atom loss since the metastable states do not interact with the cooling light and the fraction of atoms which are not magnetically trapped will drift away. The lowest-energy odd-parity states with $J = 15/2,13/2,11/2,9/2$ are fine-structure levels of the ground term. They decay via magnetic dipole transitions which have been calculated in the LS coupling approximation. The resulting lifetimes indicated in Fig. 1 range from 0.02 to 0.24 s. Also the lowest-energy even-parity states with $J = 17/2,19/2,21/2$ are expected to be long-lived, but with lifetimes that are unknown.

Measurements of the MOT number decay curve with the slowing beam turned off showed no indication of fast two-body loss ($\beta \approx 0$). The MOT lifetime was found to range from 10 to 43 ms as the detuning was scanned from -5 to -50 MHz. Representative decay curves are shown in Fig. 3. Fitting Eq. (4) to the data with $\rho_{\rm ee}$ determined from Eq. (1) we found $\gamma_{\rm bg} \simeq 1 \pm 1\,{\rm s}^{-1}$ and $\gamma_{\rm ms} + \gamma_{\rm la} \simeq 300.0 \pm 100.0\,{\rm s}^{-1}$. The value for $\gamma_{\rm la}$ is unknown, so the value of 300.0 $\rm s^{-1}$ should be taken as an upper limit on the scattering rate into metastable loss states. This value is much larger than those reported for Yb [25] and Tm [4] but is much smaller than the value reported for ^{165}Ho [6] ($\gamma_{\rm ms} = 1510\ {\rm s}^{-1}$). The Ho measurements in [6] were taken with a much higher background pressure, mainly He, which might contribute to the discrepancy. The branching ratio to metastable states is in any case very small, $\gamma_{\rm ms}/(\gamma + \gamma_{\rm ms}) \sim 10^{-6}$, so that loss out of the cycling transition is dominated by Raman transitions to other ground hyperfine levels with a branching ratio we estimated above to be $\sim 10^{-5}$. On the basis of these measurements we conclude that it should be possible to make high-fidelity hyperfine-state-resolved measurements of Ho atoms, which will be important for qubit experiments.

In conclusion, we demonstrated a magneto-optical trap of Ho atoms. Single-frequency molasses light together with a slowing beam is sufficient to load a MOT with as many as 10^5 atoms at temperatures below 100 μK from an atomic beam source. The atoms are prepared in the $F_g = 11$ level with a probability of $\sim$99%, and fractional leakage rates out of the cooling transition are $\sim 10^{-5}$. Future work will explore the use of this cold sample as the starting point for quantum control experiments which take advantage of the large manifold of hyperfine states.

This work was supported by NSF Grant No. PHY0969883 and the University of Wisconsin graduate school. We are grateful to J. Covey, J. Nipper, and H. Gorniaczyk for contributions at early stages of this experiment, and we thank B. Hemmerling from the Doyle group for helpful discussions concerning measurements of the metastable decay rate.

[1] K. Honda, Y. Takahashi, T. Kuwamoto, M. Fujimoto, K. Toyoda, K. Ishikawa, and T. Yabuzaki, Phys. Rev. A **59**, R934 (1999).

[2] J. J. McClelland and J. L. Hanssen, Phys. Rev. Lett. **96**, 143005 (2006).

[3] M. Lu, S. H. Youn, and B. L. Lev, Phys. Rev. Lett. **104**, 063001 (2010).

[4] D. Sukachev, A. Sokolov, K. Chebakov, A. Akimov, S. Kanorsky, N. Kolachevsky, and V. Sorokin, Phys. Rev. A **82**, 011405(R) (2010).

[5] J. Miao, J. Hostetter, G. Stratis, and M. Saffman, Bull. Am. Phys. Soc. **58**, U2.00005 (2013).

[6] B. Hemmerling, G. K. Drayna, E. Chae, A. Ravi, and J. M. Doyle, arXiv:1310.3239.

[7] M. Lu, N. Q. Burdick, S. H. Youn, and B. L. Lev, Phys. Rev. Lett. **107**, 190401 (2011).
[8] M. Lu, N. Q. Burdick, and B. L. Lev, Phys. Rev. Lett. **108**, 215301 (2012).
[9] K. Aikawa, A. Frisch, M. Mark, S. Baier, A. Rietzler, R. Grimm, and F. Ferlaino, Phys. Rev. Lett. **108**, 210401 (2012).
[10] K. Aikawa, A. Frisch, M. Mark, S. Baier, R. Grimm, and F. Ferlaino, Phys. Rev. Lett. **112**, 010404 (2014).
[11] E. Brion, K. Mølmer, and M. Saffman, Phys. Rev. Lett. **99**, 260501 (2007).
[12] M. Saffman and K. Mølmer, Phys. Rev. A **78**, 012336 (2008).
[13] M. Saffman, T. G. Walker, and K. Mølmer, Rev. Mod. Phys. **82**, 2313 (2010).
[14] A. Kramida, Y. Ralchenko, J. Reader, and NIST ASD Team, NIST Atomic Spectra Database, version 5.1, http://physics.nist.gov/asd.
[15] V. N. Gorshkov and V. A. Komarovskii, Opt. Spectrosk. **47**, 631 (1979) [Opt. Spectrosc. (USSR) **47**, 350 (1979)].
[16] E. A. D. Hartog, L. M. Wiese, and J. E. Lawler, J. Opt. Soc. Am. B **16**, 2278 (1999).
[17] G. Nave, J. Opt. Soc. Am. B **20**, 2193 (2003).
[18] L. S. Goodman, H. Kopfermann, and K. Schlüpmann, Naturwissenschaften **49**, 101 (1962).
[19] B. K. Newman, N. Brahms, Y. S. Au, C. Johnson, C. B. Connolly, J. M. Doyle, D. Kleppner, and T. J. Greytak, Phys. Rev. A **83**, 012713 (2011).
[20] H. J. Metcalf and P. van der Straten, *Laser Cooling and Trapping* (Springer, New York, 1999).
[21] J. Dalibard and C. Cohen-Tannoudji, J. Opt. Soc. Am. B **6**, 2023 (1989).
[22] S. H. Youn, M. Lu, and B. L. Lev, Phys. Rev. A **82**, 043403 (2010).
[23] D. Sesko, T. Walker, C. Monroe, A. Gallagher, and C. Wieman, Phys. Rev. Lett. **63**, 961 (1989).
[24] J. E. Bjorkholm, Phys. Rev. A **38**, 1599 (1988).
[25] T. Loftus, J. R. Bochinski, R. Shivitz, and T. W. Mossberg, Phys. Rev. A **61**, 051401 (2000).